Tests of Gravity at the 100 Micron Scale and Below

Joshua Long
Indiana University Cyclotron Facility, Bloomington, IN, USA

Experimental limits allow for new forces in nature millions of times stronger than gravity at distance scales resolvable to the unaided eye, and trillions of times stronger than gravity at scales accessible to scanning probe microscopy. Recent theoretical work has led to specific predictions of new physics in these regimes, including possible signatures of extra spacetime dimensions. This presentation will review several experiments and proposals designed to be sensitive to new physics at these scales, with emphasis on an experiment in progress at Indiana University that probes the range from about 10 to 100 microns.

1. INTRODUCTION

This presentation focuses on a series of table-top sized experiments designed to be sensitive to gravity and possible new physics at distance scales below 100 μm, with emphasis on an experiment in progress at Indiana University. This experiment is a continuation of one recently completed in the laboratory of Prof. John Price at the University of Colorado. The treatment is at the introductory level, and concentrates on experimental techniques and the sensitivity attainable with them.

The first sections include a description of the parameters in terms of which these experiments commonly report their results, and a number of specific predictions of new effects these experiments can test. Following sections describe the experiments, starting with those sensitive in the range above a few microns. These include classical gravity measurements carried out with torsion pendulums, which are the most sensitive at 100 μm. Recently, experiments using high-frequency techniques (including the Colorado-Indiana project) have attained the most sensitivity at the short-distance end of this range. The final sections discuss experiments and proposals sensitive to the range below 1 μm, where the dominant background is the Casimir force. The presentation focuses mainly on active programs that have published results, and also highlights efforts at Stanford, the host institution of this conference, which has played a major role in both theoretical and experimental work in this field.

2. PARAMETER SPACE

Short-range experiments are designed to be sensitive to new physics that manifests itself as a deviation from the Newtonian inverse-square law. The most popular parameterization of these deviations in the literature is in terms of the Yukawa potential, given by:

$$V(r) = \frac{Gm_1m_2}{r}\left(1 + \alpha e^{-r/\lambda}\right) \tag{1}$$

where G is the Newtonian Gravitational Constant, m_1 and m_2 are test masses, and r is their separation. The first term is the potential due to standard gravity and the second is the Yukawa potential. Here, α is the strength of a new interaction relative to gravity and λ is the range. The Yukawa interaction arises when the force between the test masses is mediated by a massive field; the range λ is given by the Compton wavelength of the mediating particle. In the absence of a signal of a new interaction (no such verifiable signal has been observed in any short range experiment to date), experimental results are commonly reported in terms of limits on the strength parameter α for a given range λ. They

are often displayed on a log-log plot of one parameter versus the other, of which there are several examples in this presentation.

3. EXISTING LIMITS AND THEORETICAL MOTIVATION

Fig. 1 is the first example. It shows the experimental limits in 1998, just after the Colorado project began, along with some theoretical predictions. Here, the range λ runs from 1 μm to 1 cm, the strength α runs from 10^{-6} times gravitational strength up to 10^{10}. The experimentally excluded area is above and to the right of the solid black curves; each curve represents a 90% C. L. upper limit on α with the exception of the curve labeled "Irvine", which is a 1σ upper limit. All of the limits are derived from torsion pendulum experiments. The Irvine curve is the result from an experiment in which a cylindrical test mass was suspended inside a long tube, nominally a null geometry for $1/r^2$ forces [1]. The curve labeled "Mitrofanov" is the result of a miniature version of the Cavendish experiment [2]. The curve labeled ``Lamoreaux" derives from an experiment in which a torsion balance was used to measure the Casimir force between a spherical shell and flat disk [3]; the limits on new forces consistent with the experimental residuals of this experiment are derived in Refs. [4] and [5]. The experimental limits show that as of 1998, gravity itself had only been measured to length scales of about 1 mm. The limits allowed for new forces in nature several million times stronger than gravity at ranges of about 10 μm.

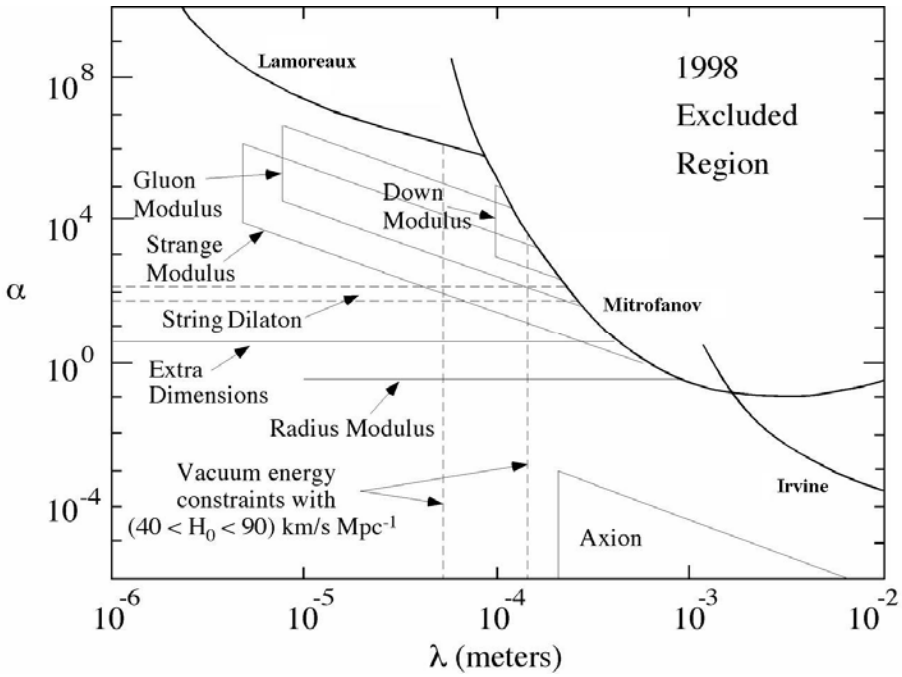

Figure 1: Parameter space for short-range experiments in which the strength α of a hypothetical Yukawa interaction is plotted vs. the range λ.

In addition to this very general motivation for new experiments, a number of specific theoretical predictions of new physics had appeared in this regime. These are represented by the fine and dashed lines in Fig. 1. Two recent comprehensive reviews on the subject can be found in Refs. [6] and [7]. The theoretical predictions tend to fall into

three broad categories: signatures of compact extra dimensions, forces arising from the exchange of exotic scalar fields, and ideas motivated by the cosmological constant problem. The horizontal line labeled "Extra Dimensions" in Fig. 1 refers to the extra dimensions of string theories. String theories are the leading candidates for a unified description of gravity and the other fundamental forces, and have to be formulated in more than 3 spatial dimensions. In the original formulations of string theory the extra dimension were taken to be compacted at lengths on the order of the Planck scale ($M_P \sim 10^{19}$ GeV or 10^{-35} m) and presumably undetectable by any practical experiment. In 1998 a class of models was discovered in which the weakness of gravity relative to the other fundamental forces is explained by two or more of these extra dimensions remaining large and accessible only to gravity; the spreading of the gravitational interaction into the extra dimensions appears to dilute its strength. The original model, termed the ADD model after its authors [8], relates the size R of the extra dimensions to their number n according to the expression:

$$R^n = M_P^{\,2} / M^{*(2+n)} \quad , \tag{2}$$

Where M^* is the actual scale of the gravitational interaction. Assuming the weak scale M_W to be the only short-distance scale in nature (and effectively eliminating the hierarchy problem), choosing $M^* \sim M_W \sim 1$ TeV in Eq. 2 yields $R \sim 1$ mm for $n = 2$. The consequence is that gravitational experiments approaching this range should be sensitive to potentials dictated by the appropriate Gauss' law in 5 spatial dimensions, or forces varying as r^{-4}. Detailed phenomenological investigations of these models predict Yukawa-type corrections to the Newtonian power law as the scale $R \sim \lambda$ of the extra dimensions is approached from above [9, 10]; the model in Fig. 1 predicts $\alpha = 4$ for $n = 2$. The scale M^*, now a free parameter in these models, need not be fixed at 1 TeV; the range of the prediction in Fig. 1 represents a variation in the scale from about 1 TeV at $\lambda \sim 1$ mm to 20 TeV at $\lambda \sim 1$ μm.

Scalar fields giving rise to new forces include moduli, dilatons, and axions. Moduli are gravitationally-coupled scalars that parameterize the size and shape of extra dimensions in string theories. They can acquire masses in the meV range via a number of scenarios, whereby they are predicted to mediate forces in the range of a few microns with a wide range of couplings [11, 12]. The dilaton is another scalar in string theory, the vacuum expectation value of which determines the strength of the interaction between strings. The coupling of the dilaton has been estimated to lie in a wide range above gravitational strength, but the mass has been constrained only by experiment [13, 14]. The axion is a light pseudoscalar field intended to explain the apparent absence of CP-violating effects in strong (QCD) interactions. It is also predicted to mediate sub-millimeter range forces between unpolarized test masses, though at an extremely feeble level [15, 16].

Finally, another class of predictions arises in attempts to address the cosmological constant (Λ) problem, the vast discrepancy between the observed curvature of the universe and the amount expected from vacuum energy contributions of the standard model fields. The vertical bars in Fig. 1 arise from models that postulate new fields with interaction ranges on the order of $\Lambda^{-1/4} \sim 100$ μm that act to suppress the vacuum contributions [17, 18].

4. EXPERIMENTAL CHALLENGES

With all of this motivation for short-range tests of gravity in the late 1990s, it may strike as odd why a number of experiments did not begin publishing right away. After all, the Cavendish experiment, published in 1798, represented a very sensitive measurement of Newton's Constant with test mass separations of a few centimeters. The principle

challenge to gravitationally sensitive experiments at short range is the scaling of the signal force with the size of the test masses. If all dimensions of the test masses are scaled by the same factor L, the signal varies as L^4 and becomes extremely small at short ranges. For example, the gravitational force between spherical test masses with size and separation L is approximately $G\rho_1\rho_2L^4$, where ρ_1 and $\rho_2$are the mass densities. Substituting typical heavy metal densities (~ 20 g cm^{-3}) and a scale characteristic of the Cavendish experiment (L ~ 5 cm) yields a force of about 10^{-5} N. To attain gravitational sensitivity at 100 μm, however, the experimenter is faced with scaling the test masses to that range, so as not to be overwhelmed by the Newtonian attraction at larger scales. Setting L ~ 100 μm yields F ~ 1 fN, explaining in large part why it has taken some time to complete gravitational measurements below 1 mm. At the same time, experimental backgrounds increase rapidly at short range; electrostatic forces from surface potentials scale as r^{-2}, and dipole-dipole forces from magnetic contaminants scale as r^{-4}. The following sections will discuss some experiments and proposals that have been designed to meet the dual challenge of small signals and rapidly increasing backgrounds at 100 μm and below.

5. EXPERIMENTS IN THE RANGE FROM 1-100 MICRONS

5.1. The Eot-Wash Torsion Pendulum Experiment

The extremely sensitive and highly linear response of thin fibers under tension has made the torsion pendulum the instrument of choice for laboratory gravity measurements, starting with the Cavendish experiment. The shortest-ranged gravitationally-sensitive experiment to date is the Eot-Wash Torsion pendulum experiment, an early concept of which is shown in Fig. 2 [19]. The force-sensitive detector consists of an aluminum annulus with an array of ten equally-spaced holes. The force-generating or source mass consists of a stack of flat copper disks, each a few millimeters thick, with similar arrays of holes. The source is bought into close proximity of the pendulum and rotated approximately once every 2 hours. Torques associated with gravity and possible new forces are thus modulated at 10 times the rotation frequency, which is advantageous for suppressing vibration backgrounds associated with the drive. Furthermore, the array of holes on the lower source disk is offset relative to the holes on the top, an arrangement that tends to cancel the torque associated with the long-range Newtonian attraction between the test masses but leaves shorter-range forces unaffected. Not shown in Fig. 2 is a 20 μm thick copper membrane stretched on a frame between the test masses, essential for suppressing electrostatic backgrounds.

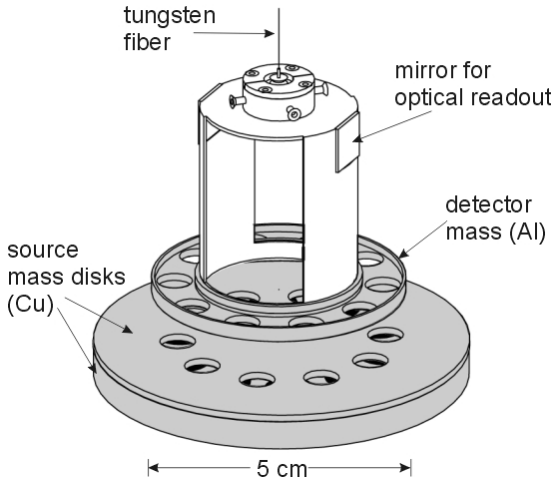

Figure 2. Eot-Wash torsion pendulum experiment (early concept). Source: [19]

A later version of this experiment attained test mass separations as low as 140 μm. Excellent agreement was obtained between the observed torque and the Newtonian predictions; the residuals on comparison with the predictions are consistent with zero, and with torque sensitivities on the order of a few fN-m. From these results, the experiment has been able to rule out Yukawa-type forces of gravitational strength and above for interaction ranges greater than about 200 μm, as shown in Fig. 8. It set a model-independent upper limit on the size of any large extra dimension of 160 μm and, for the ADD scenario with 2 large extra dimensions of equal size, it has set an upper limit of 130 μm, corresponding to a lower limit of 1.7 TeV on the unification scale of gravity [20]. The Eot-Wash group is continuing to make improvements to the experiment, including denser test masses with a larger number of smaller-sized holes to increase the Yukawa signal. A recent version of the apparatus is able to probe test mass separations below 100 μm.

5.2. High-Frequency Experiments

5.2.1. The Colorado-Indiana Torsional Oscillator Experiment

Though the torsion pendulum technique is attractive from the point of view of ultimate sensitivity, it tends to be limited by backgrounds including vibrations, tilts, temperature drifts, and mechanical relaxations, most of which would be exacerbated at small test mass separations. The Colorado-Indiana experiment takes a different approach, using high-frequency mechanical oscillators that show potential for reaching greater sensitivity at short ranges. The experiment uses a resonant detector mass with a source mass driven on resonance for maximum signal.

The experimental test masses are shown in Fig. 3 [22]. Planar geometry is used to concentrate as much test mass density as possible at the distance range of interest. The source mass consists of a tungsten reed (density ~ 20 g cm^{-3}), 4 cm long and 250 μm thick. It is driven by an actuator made from a piece of piezoelectric ceramic attached near a node. The detector mass consists of two 250 μm thick coplanar tungsten rectangles joined along their central axes by a short segment. In the 1 kHz resonant mode of interest, the rectangles counter-rotate about the axis defined by the segment. The planar geometry is nominally null with respect to r^{-2} forces, which is effective in suppressing the Newtonian background relative to new short-range effects. Electrostatic and acoustic backgrounds are suppressed with a stiff

conducting shield between the test masses. In the first version of the experiment, the shield consisted of a 60 μm thick gold-plated sapphire wafer. A gravitational strength Yukawa force between the test masses in this geometry is about 10^{-14} N, for a source-detector gap of 100 μm. This is about a factor of 10 higher than the expected Newtonian force.

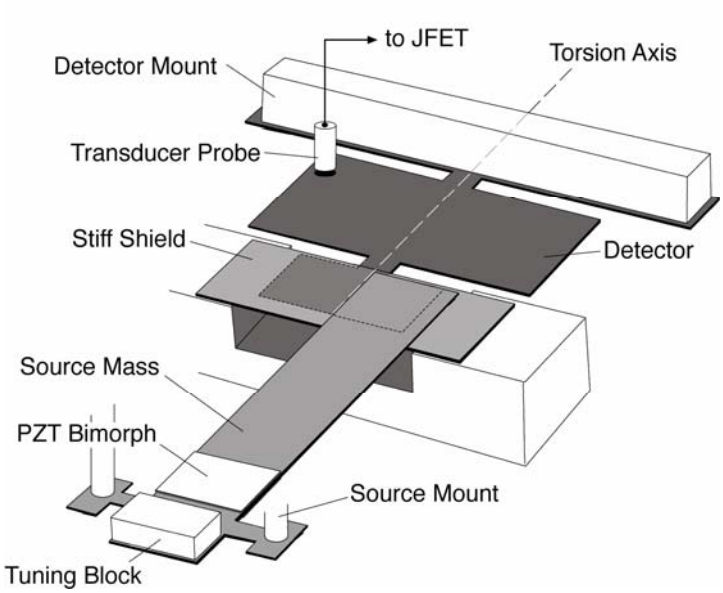

Figure 3. Sketch of the test masses in the Colorado-Indiana torsion oscillator experiment. Source: [22].

Operation of the experiment at the detector resonant frequency, while increasing sensitivity, places a heavy burden on vibration isolation. The amount of attenuation required can be estimated by comparing the inertial force associated with the motion of the source mass to a gravitational strength Yukawa force between the test masses at 100 μm; the ratio is about 10^{13}. At the operational frequency of 1 kHz it is possible to construct a simple passive vibration isolation system. In this system (not shown in Fig. 3), the source and detector masses are each mounted to the bottom stage of a series of massive (brass) disks connected by fine wires under tension. The vibration isolation stacks, called Taber isolators after their inventor at Stanford, were originally developed for large resonant-bar gravitational wave antennas. They are clearly visible in Fig. 4, which shows a photograph of the central apparatus. The attenuation Z attainable in all degrees of freedom (3 translational plus 3 rotational) for a given stack can be estimated from the expression $Z \sim (\omega/\omega_0)^{2n}$, where ω is the highest resonant frequency of a single stage, ω_0 is the operational frequency, and n is the number of stages. It is straightforward to obtain $\omega \sim 100$ Hz, so that a 5-stage isolator provides an attenuation of about 10^{-10} [23]. Suspending both source and detector masses from these isolators thus provides an attenuation of 10^{-20}, so that the experiment is nominally over-designed in terms of the expected vibration background. The vibration isolation stacks are mounted to inverted micrometer stages fixed to the top plate of the apparatus, allowing full 3-axis position control of the test masses. The central apparatus in Fig. 4 is covered by a 75-liter bell jar and is maintained at a pressure of 10^{-7} torr to further reduce acoustic backgrounds.

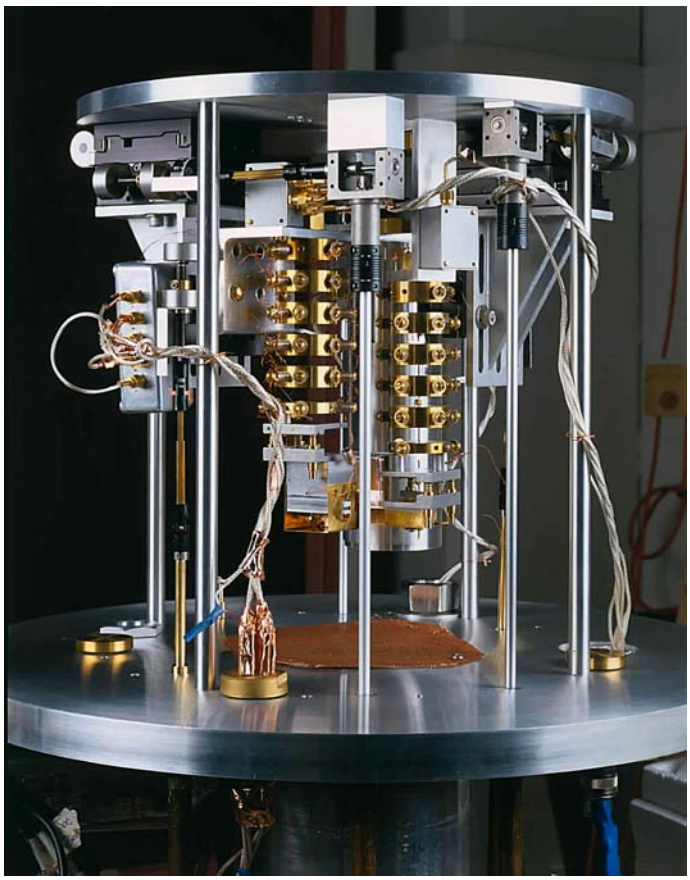

Figure 4. Central apparatus of Colorado-Indiana experiment. The distance from the base plate to the top plate is about 50 cm.

A series of runs in 2002 yielded no experimental evidence of any resonant signal, nor any vibration, electromagnetic, or acoustic backgrounds. The only effect observed was noise associated with the thermal motion of the atoms in the bulk of the detector mass. This is the mechanical analogue of Johnson noise in a resistor. In this limit, the approximate force sensitivity is given by:

$$\alpha \sim \frac{1}{G\lambda^2 \rho_s \rho_d A_d} \sqrt{\frac{kTm\omega}{Q\tau}} \tag{3}$$

Where A_d is the detector area, k is Boltzmann's constant, T is the temperature, ω is the detector resonant frequency, Q is the detector mechanical quality factor, and τ is the integration time. This expression is similar for other thermal-noise limited experiments, differing by factors related to the test mass geometry. To reduce the thermal background, the detector mass had been annealed for several hours before installation in the experiment. The annealing process, in which the detectors are heated to about 1600 K and slowly cooled, is thought to lead to higher Qs by promoting the growth of larger crystal grains in the tungsten, which in turn reduce the mechanical damping. For the detector used in the experiment, annealing increased the Q from about 5×10^3 to 2.5×10^4. In the 2002 run the integration time was approximately 1 day, corresponding to a force sensitivity of about 2 fN. Eq. 3 with these values and T = 300 K, $\omega = 2\pi \times 1000$ Hz closely approximates the limits at large λ on additional Yukawa-type forces obtained from a likelihood analysis accounting for uncertainties in the test mass metrology [22]. These limits are presented in Fig. 8. At the time

of publication, this curve represented the most sensitive limit in the range between 10 and 1000 μm, improved on previous limits by as much as three orders of magnitude, and set the most stringent lower bound on the mass of the dilaton at 9 meV.

Given the high sensitivities attained by the Eot-Wash experiment at larger ranges, subsequent development of the torsion oscillator experiment at Colorado and more recently at Indiana University has focused on attaining better sensitivity in the range below 100 μm. In the published experiment, the 100 μm test mass separation is determined largely by the shield thickness (60 μm). The equilibrium positions of the test masses can be set such that the gaps between either mass and the shield can be made consistently less than 20 μm. This is presumably made possible in large part by the high bending stiffness of the vibration isolation stacks. At 50 μm test mass separation, the electrostatic and acoustic backgrounds are estimated to be about 4 orders of magnitude larger than the thermal noise background at room temperature, and a thermal noise limited experiment should be possible if a 10 μm shield could be found with sufficiently low compliance (~10^{-3} m N^{-1} or less). An estimate of the compliance of a 1 cm^2 sapphire plate 10 μm thick clamped at two ends gives a value in this range. Taking a hint from the Eot-Wash experiment, however, a similar calculation for a metal membrane stretched to its yield point results in a reduction in the compliance by about two orders of magnitude.

Fig. 5 shows a sketch (elevation view) of a new shield prototype for the Indiana experiment. The shield consists of a 10 μm thick beryllium copper foil stretched over a frame that can be pried apart with a screw. A plan view would show that the foils used have a hyperbolic profile. Initial tests with rectangular foils resulted in buckling along the free edges; the hyperbolic shape is much more effective in distributing the tension along the direction perpendicular to the stretching. Measurements of the surface profile of the prototype revealed surface variations with a 3 μm peak-to-peak maximum. Measurements of the compliance, made by hanging weights from either end of a wire stretched across the midline of the foil, yielded in a maximum value of 3 ×10^{-5} m/N in accordance with the estimate.

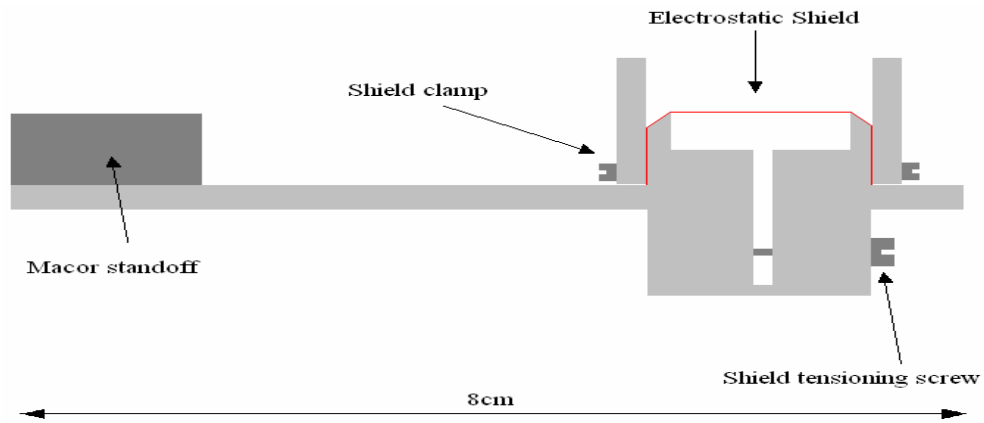

Figure not to scale

Figure 5. Stretched membrane shield prototype in Colorado-Indiana experiment.

In an attempt to gain some additional sensitivity while still at room temperature, new detector masses have been prototyped for the experiment. The composition and dimensions are the same, but they have been annealed at higher

temperatures in an attempt to get higher *Q*s. The annealing temperature, 2700 K, is about 100 K higher than a secondary re-crystallization threshold in tungsten. As expected, the samples annealed at higher temperatures exhibit significantly larger grains than previously observed. Grain sizes of up to 90 μm are observed, as shown in Fig. 6; the previous record was about 15 μm. The mechanical properties of the new detectors have yet to be measured, though previous studies in the literature suggest that an additional factor of 5 improvement in the *Q* can be expected [24]. With the stretched membrane shield and modest improvements in the detector *Q*, the projected sensitivity of the Indiana experiment is expected to improve by as much as two orders of magnitude in the range near 20 μm.

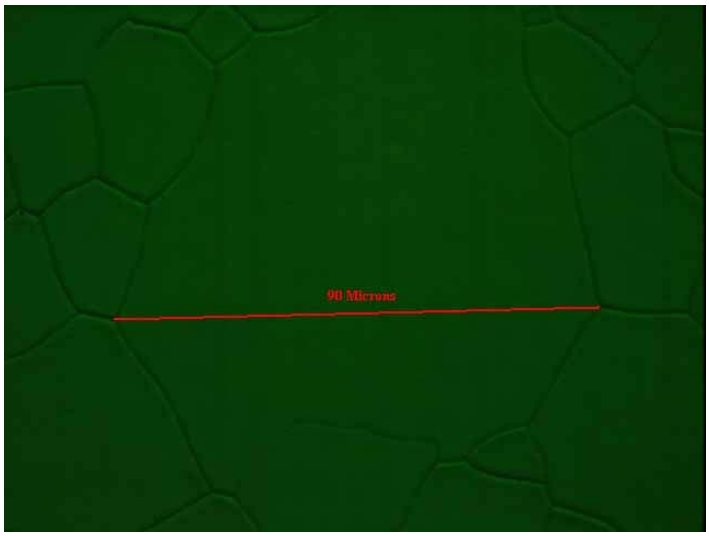

Figure 6. Micrograph of detector prototype for Colorado-Indiana experiment, showing crystal grain 90 μm wide.

5.2.2. The Stanford Micro-cantilever Experiment

As shown in Fig. 8, significant additional parameter space below 100 μm has been covered since 1998. The current best limits between 2 and 20 μm derive from an experiment at Stanford, in a group led by Aharon Kapitulnik. This is also a high frequency experiment, but on a much smaller scale than the Colorado-Indiana project. A schematic of the apparatus is shown in Fig. 7.

The test mass consists of a gold cube, approximately 50 μm on a side, mounted on the end of a silicon nitride cantilever 250 μm long. Instead of modulating the gap between the source and detector, this experiment modulates the mass. The drive mass consists of alternating strips of high and low density materials, in this case silicon and gold. This array is driven horizontally such that the density of the strips modulates at the fundamental cantilever resonant frequency. The frequency of the drive mechanism can thus be set to a sub-harmonic of the cantilever response, putting less of a burden on vibration isolation.

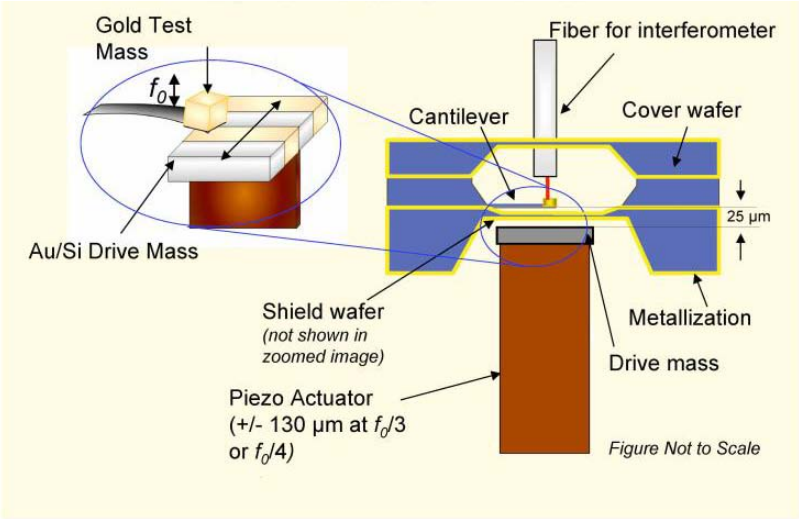

Figure 7. Sketch of the Stanford micro-cantilever experiment. Figure courtesy Sylvia Smullin [25].

The complete central apparatus in Fig. 7 consists of a 3-tiered wafer stack, with the central wafer supporting the detector cantilever. The bottom wafer comprises the electrostatic shield, a 3 μm thick silicon nitride plate with a 100 nm gold coating. Using this geometry the experiment is able to probe test mass separations in the 20 μm range.

To reduce the thermal noise background, this experiment is run at cryogenic temperatures. With the masses mounted at the tip, typical cantilevers in this experiment have resonant frequencies of about 300 Hz and *Q*s of about 4×10^4. At the operational temperature of about 10 K the expected limiting thermal noise is in the attonewton range for hour-long integration times. The apparatus in Fig. 7 is mounted onto a probe and inserted into a helium cryostat. A passive vibration isolation system, consisting of 2 stages with resonant frequencies of about 2.5 Hz, separates the drive mass and cantilever mounts and provides an attenuation of about 10^{-8} at the cantilever response frequency.

Data from the experiment published in 2003 [26] showed evidence of a resonant signal a small numerical factor above the measured thermal noise background. This was attributed to motion of the electrostatic shield coupling to the test mass, caused in turn by electrostatic interactions with surface variations on the drive mass strips. Using these data, the Stanford group was able to set the experimental limits labeled “Stanford 1” in Fig. 8.

Since the first publication, several improvements have been made to the apparatus. These include more precise test mass alignment to reduce errors associated with a predicted Yukawa signal, and the addition of a conducting top layer to the drive mass strips in order to reduce electromagnetic coupling. A series of runs in 2004 detected a small signal a few aN above the limiting thermal noise, possibly due to mechanical or electrical coupling between the drive mass actuator and the experimental readout. However, the expected modulation (in the presence of a Yukawa force) of the signal phase relative to the equilibrium position of the drive mass strips was not observed, and the results were used to set additional limits [27]. These limits, labeled “Stanford 2” in Fig. 8, improved on the previous results by up to an order of magnitude in the range from 6-20 μm.

Additional sensitivity could be expected with reduction of the coupling between the drive and readout, and with further improvement in the precision of the horizontal alignment of the drive mass. A second-generation micro-cantilever experiment in the Stanford group, using larger-area drive masses embedded in the top surface of a

hemispherical rotor, could yield another order of magnitude improvement in the experimental sensitivity in the 10-100 μm range [27, 28].

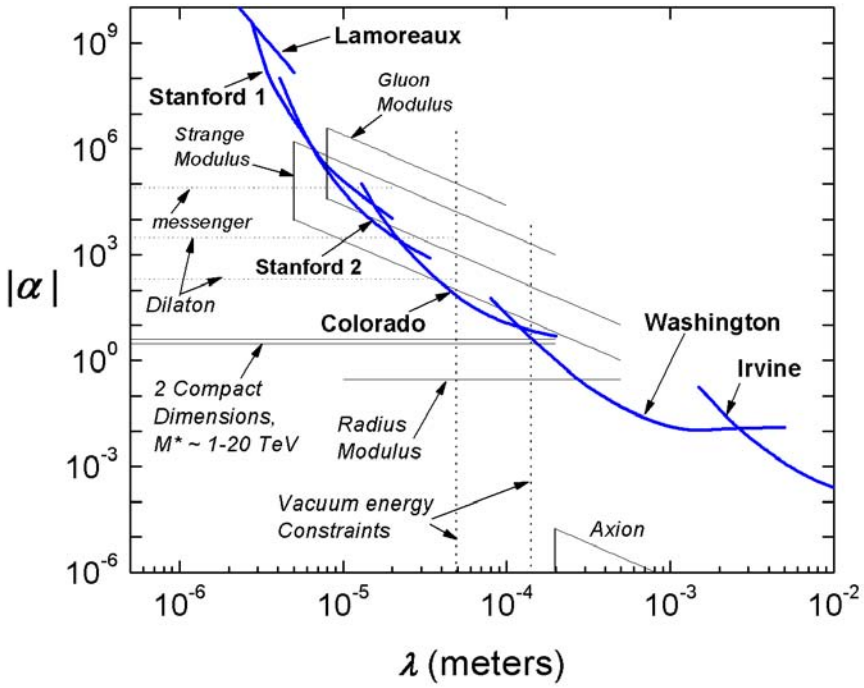

Figure 8. Experimental limits and predictions in the range from 0.5 μm to 1 cm as of late 2005. Adapted from [21].

At least two additional experimental programs are active in the range above a micron. These include a cryogenic low-frequency null-geometry experiment at the University of Maryland with a projected sensitivity as low as $\alpha \sim 10^{-3}$ at 100 μm [29], and a torsional oscillator experiment at the University of Dusseldorf with a projected room temperature sensitivity just below the Colorado result over the same range [30].

6. EXPERIMENTS BELOW 1 MICRON

6.1. Limits from Casimir Force Measurements

Fig. 9 shows the situation down to the nanometer range, with some revised predictions. In the range below 1 μm, all the experimental limits, with one exception [31], are derived from measurements of the Casimir effect, a force that arises between conductors due to zero-point fluctuations of the electromagnetic field. In these experiments, the Casimir force is measured as precisely as possible. Experiments at UC Riverside [32] used scanning probe microscopy, and an experiment in Stockholm by Ederth measured the force between microscopic crossed cylinders [33]. In separate analyses the data are then used to ascertain the largest possible Yukawa-type force that could have been present between the experimental test masses and still consistent with the residuals [34, 35].

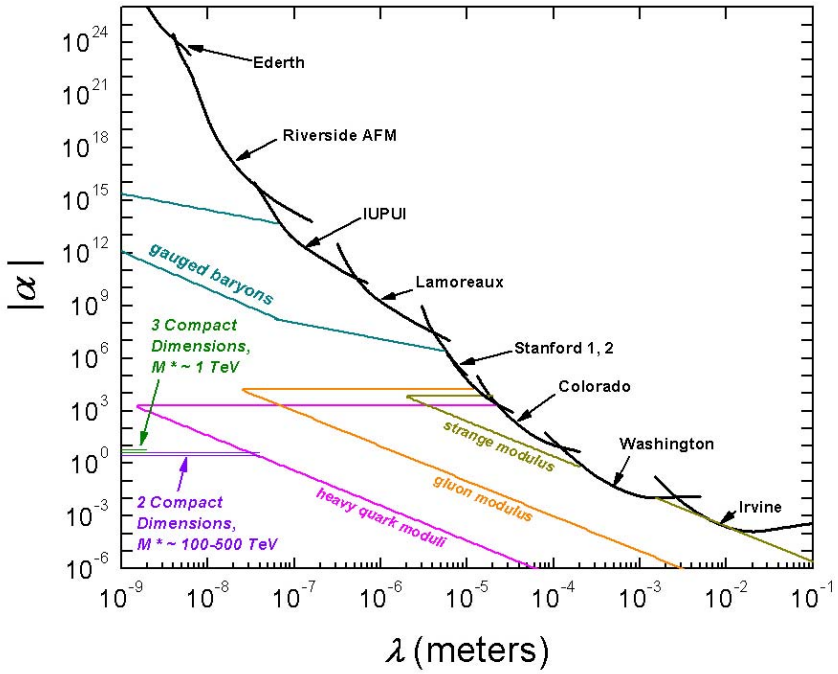

Figure 9. Experimental limits and revised predictions down to 1 nm.

Predictions for modulus forces have been extended well into this regime by a pair of Stanford physicists [36]. There are also new predictions for effects as strong as 10^{15} times gravitational strength in this regime; these forces arise in models in which additional fields, such as gauged baryons, can propagate in extra dimensions along with gravity.

6.2. Casimir Background Suppression

In the Casimir force experiments, other effects are considered backgrounds, suggesting that dedicated new force searches in the range below a micron should be able to improve the limits significantly with a modest technological investment. Above 10 μm the dominant background is the electrostatic force; torsion pendulums with shielding have been the instruments of choice here though recently the high-frequency experiments have attained more sensitivity at the lower end of this regime. Below a few microns, the Casimir force becomes significant and quickly begins to dominate. In the range between 10^{-7} and 10^{-5} m it may still be possible to use shielding techniques to handle the Casimir background, as this range is still above that of the plasma wavelength (λ_P) of the (typically) conducting test masses in these experiments. Below 10^{-7} m, direct shielding can no longer be effective and other techniques, including neutron experiments [37], have been proposed to improve limits this range.

One possible implementation of shielding in the sub-micron range is sketched in Fig. 10. A flat metallic sample with alternating thicknesses D and 2D, mounted on a dielectric substrate, is scanned beneath a metallic probe suspended a distance D above. Since the electromagnetic modes responsible for the Casimir interaction can only penetrate a distance on the order of λ_P into the sample, maintaining $D > \lambda_P$ ensures that the Casimir force on the probe due to the sample will be independent of its horizontal position. This will not be true of mass-coupled forces with ranges on the on the order of D or greater. As D drops below λ_P, the modes begin to penetrate the sample and the probe will sense a

difference in force between the two sides due to the Casimir interaction. This effect is exploited, for example, in the improved drive mass of the Stanford micro-cantilever experiment to reduce possible long-range Casimir backgrounds. Using a technique for calculating Casimir forces between metals of finite conductivity and thickness [38], the Colorado group has calculated the difference in force between the probe in Fig. 10 and sample regions of thickness D and 2D, for various values of D, and then compared this result to the difference in the Yukawa force for the same geometry with λ = D [39]. Requiring a signal-to-background ratio of unity yields the curve labeled "buried mass" in Fig. 13.

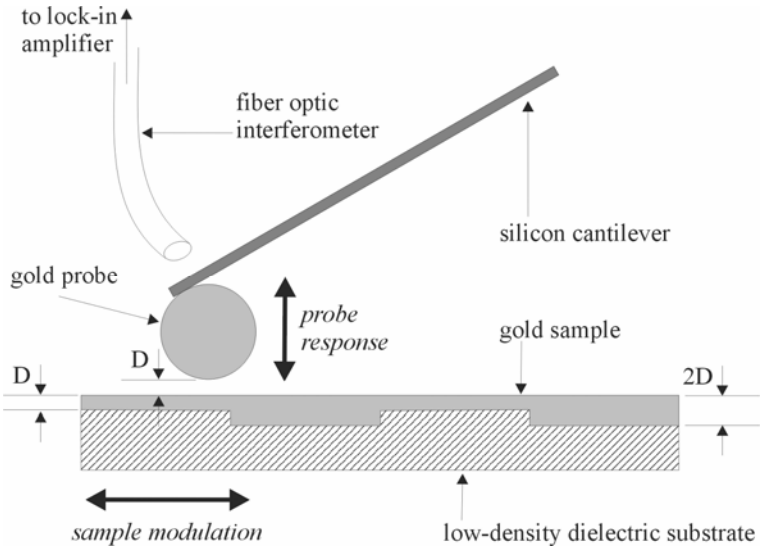

Figure 10. Proposed scanning probe microscopy experiment. The approximate scales are explained in the text.

6.2.1. Indiana-Purdue Iso-electronic Experiment

Since the publication of this calculation, an Indiana-Purdue group has made considerable progress on an experiment using similar principles. In this experiment, a gold-plated sapphire sphere is scanned over the surface of a composite sample. A schematic view is shown in Fig. 11. The sample consists of 200 nm thick coplanar strips of gold and germanium, plated with a common gold top layer. The top layer thickness is 150 nm, nominally 15 nm greater than λ_P of the gold. The composite sample is attached to the edge of a high quality micro-electromechanical torsional oscillator, parallel to the torsion axis. The experiment is performed by moving the sphere back and forth across the gold-germanium interface of the sample, while monitoring the resonance of the mechanical oscillator. The resonance shifts in the presence of the external force gradient induced by the Casimir interaction; differences in forces between the probe and either side of the composite are measured by monitoring the resonance shift as the probe crosses the gold-germanium interface.

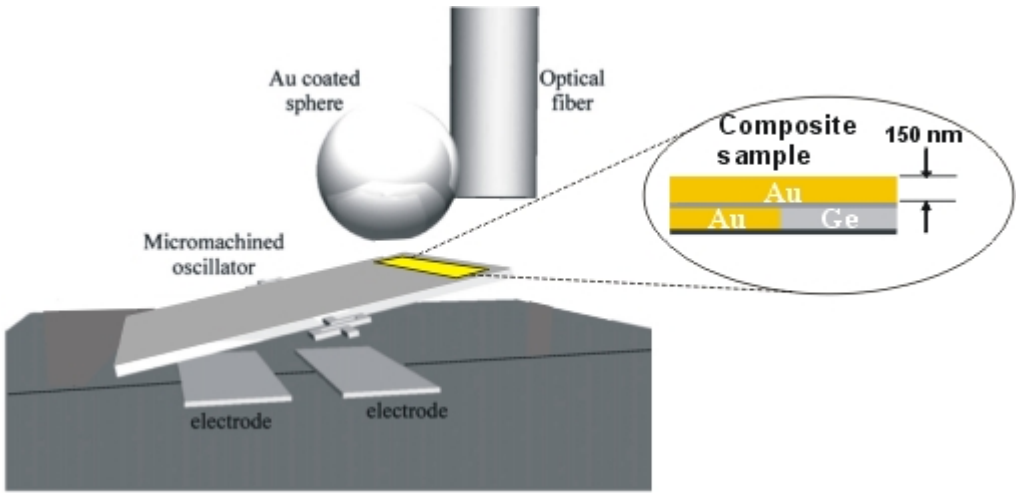

Figure 11. Sketch of the test masses in the Indiana-Purdue iso-electronic experiment. The width of the micro-machined oscillator is approximately 1 mm. Adapted from [31].

Data from this experiment published in 2005 show clear evidence of a force difference, ranging from about 1 fN at 500 nm test mass separations to 5 fN at 100 nm. The resolution is high enough to rule out an exponential relationship between the force and separation, and the authors are able to use these data to set limits on Yukawa-type interactions, labeled "IUPUI" in Fig. 9 [31]. While the exact force-to-distance relationship cannot be derived from the data, the magnitude of the signal is consistent with a Casimir force difference arising from a 0.1 nm step in the top gold layer coincident with the underlying interface.

6.2.2. Experiments and Proposals with Trapped Atoms

Also since the publication of the calculation in Ref. [39], Stanford researchers have pointed out that even greater suppression of Casimir backgrounds in sub-micron experiments could be attained by replacing at least one of the conducting test masses with a dielectric [36]. In a possible realization of this scenario, shown in Fig. 12, the authors proposed replacing the conducting probe with a cloud of Bose-condensed (BEC) ^{87}Rb atoms. In this proposal, 2 BEC (with atomic density of about 10^{18} cm^{-3} and dielectric constant $\varepsilon \sim 1$) are trapped at the nodes of a laser reflected off a flat conducting surface. The surface also acts as a Casimir shield for a modulated-mass source behind it. The laser determines the test mass separation, here about 400 nm. The atomic wave functions of the clouds acquire different phase shifts depending on the interaction potentials with the surface. The Casimir portion of this phase is determined only by the conducting shield if the latter is sufficiently thick, nominally on the order of λ_P of the shield material. Any phase shift due to the Yukawa interaction with the source mass can be probed by changing the density of the portion immediately behind the shield.

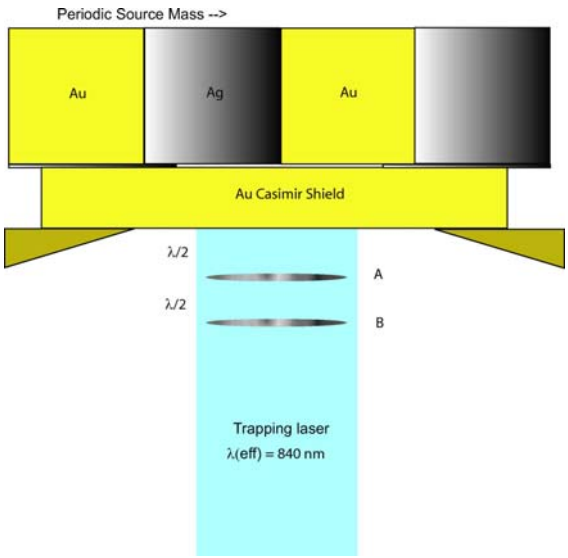

Figure 12. Schematic view of proposed Stanford BEC Experiment. Trapped BEC clouds are at positions marked A and B. Source mass strips measure approximately 100 μm on a side; the Casimir shield thickness is about 200 nm. Source: [36].

An experiment in the Cornell group at JILA has measured the Casimir-Polder force between an ^{87}Rb BEC and a dielectric surface [40]. The surface-sample separation is about 5 μm, significantly larger than previously achieved. (The group also notes the inherent difficulty in trapping alkali atoms near conducting surfaces.) The data were then used to set limits on new forces. The result is labeled "JILA BEC" in Fig. 13, and while not currently competitive it suggests and upper limit of the sensitivity of this technique. The limiting sensitivity calculated in the Stanford analysis is also shown.

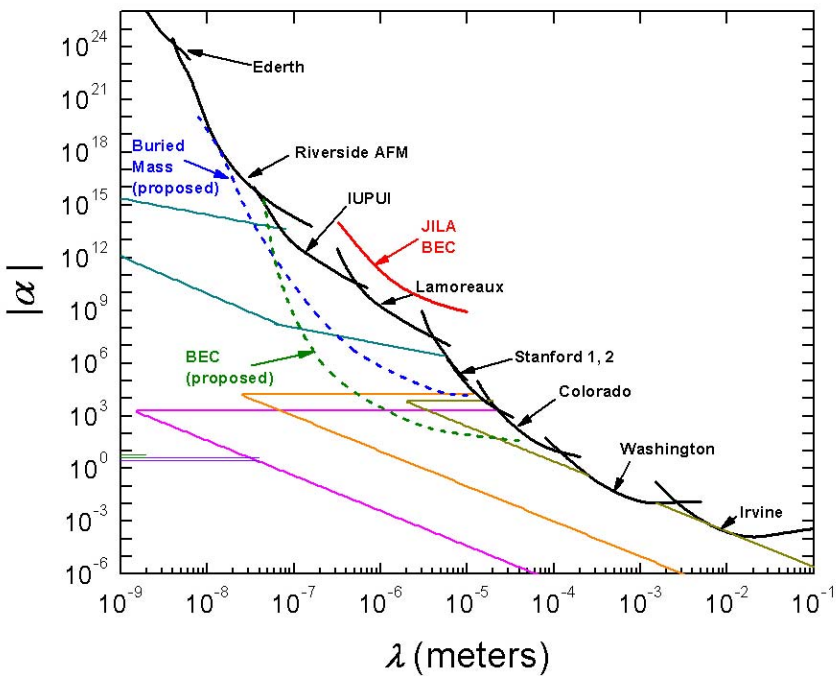

Figure 13. Parameter space with projected sensitivities of sub-micron experiments.

7. CONCLUSIONS

In summary, short-range tests of gravity have explored about 8 square decades of the Yukawa parameter space above 1 μm in the past 8 years. Several additional decades should be within reach of ongoing experiments. These include torsion pendulums and low-frequency experiments above 50 μm, and high-frequency experiments below. There is new and expanding theoretical interest in the ranges above and below 1 μm, and while the experiments cannot rule out string theory, they provide important constraints on the types of fields allowed in it. Dedicated new force searches, in addition to precision Casimir force measurements, have begun to explore the range below 1 μm. The projected sensitivities of proposals in this range suggest that up to 10 additional square decades of parameter space may be accessible in the future. Both in this range and above, of course, this depends critically on the control of the experimental backgrounds.

Ackowledgments

The author wishes to thank all of his colleagues at or previously at the University of Colorado and members of the Stanford group who provided material for this presentation, including John Price, Hilton Chan, Allison Churnside, Andrew Geraci, Eric Gulbis, Sylvia Smullin, Dominic Thurmer, Michael Varney, and David Weld. Thanks also to Brian Bartram of MST Division at Los Alamos National Laboratory for assistance with high-temperature annealing.

References

[1] Hoskins J. H., Newman R. D., Spero R., Schultz J., Phys. Rev. D 32 (1985) 3084.

[2] Mitrofanov, V. P., Ponomareva, O. I., Sov. Phys. JETP 67 10 (1988) 1963.

[3] Lamoreaux S. K., Phys. Rev. Lett. 78 (1997) 5.

[4]Long J. C., Chan H. W., Price, J. C., Nucl. Phys. B 539 (1999) 23.

[5] Klimchitskaya, G. L., et al., Int. J. Mod. Phys. A20 (2005) 2205-2221.

[6] Hewett, J., Spiropulu, M., Ann. Rev. Nucl. Part. Sci. 52 (2002) 397.

[7] Adelberger, E. A., Heckel, B. R., Nelson, A. E., Ann. Rev. Nucl. Part. Sci. 53 (2003) 77.

[8] Arkani-Hamed, N., Dimopoulos, S., Dvali, G., Phys. Lett. B 429 (1998) 263.

[9] Floratos, E. G., Leontaris, G. K., Phys. Lett. B 465 (1999) 95.

[10] Kehagias, A., Sfetsos, K., Phys. Lett. B 472 (2000) 39.

[11] Dimopoulos S., Giudice G., Phys. Lett. B 379 (1996) 105.

[12] Antoniadis, I., Dimopoulos, S., Dvali, G., Nucl. Phys. B 516 (1998) 70.

[13] Taylor, T. R., Veneziano, G., Phys. Lett. B 213 (1998) 450.

[14] Kaplan, D. B., Wise, M. B., J. High Energy Phys. 0008 (2000) 037.

[15] Moody, J. E., Wilczek, F., Phys. Rev. D. 30 (1984) 130.

[16] Rosenberg, L. J., van Bibber, K. A., Phys. Rep. 325 (2000) 1.

[17] Beane, S. R., Gen. Rel. Grav. 29 (1997) 945.

[18] Sundrum, R. J. High Energy Phys. 7 (1999) 1.

[19] Hoyle, C. D., et al., Phys. Rev. Lett. 86 (2001) 1418.

[20] Hoyle, C. D., Kapner, D. J., et al., Phys. Rev. D 70 (2004) 042004.

[21] Long, J. C., Price, J. C., C. R. Physique 4 (2003) 337.

[22] Long, J. C., et al., Nature (London) 421 (2003) 922.

[23] Chan, H. W., Long, J. C., Price, J. C., Rev. Sci. Instrum. 70 (1999) 2742.

[24] Duffy, W., J. Appl. Phys. 72 (1992) 5628.

[25] Smullin, S. J., et al., Proceedings of the SLAC Summer Institute on Particle Physics (SSI04), Menlo Park, 2004, ed. Hewett, J., Jaros, J., Kamae, T., Prescott, C., econf C040802 (2004)

[26] Chiaverini, J. et al., Phys. Rev. Lett. 90 (2003) 151101

[27] Smullin, S. J., et al., Phys. Rev. D 72 (2005) 122001.

[28] Weld, D. M., Private communication.

[29] Paik, H. J., Moody, M. V., Strayer, D. M., Gen. Rel. Grav. 36 (2004) 523.

[30] L. Haiberger, et al., hep-ph/0510211

[31] Decca, R. S., et al., Phys. Rev. Lett. 94 (2005) 240401

[32] Harris, B. W., et al., Phys. Rev. A 62 (2000) 052109

[33] Ederth, T., Phys. Rev. A 62 (2000) 062104

[34] E. Fischbach et al., PRD 64 (2001) 075010

[35] R. S. Decca et al., Ann. Phys. 318 (2005) 37

[36] S. Dimopoulos, A. A. Geraci Phys. Rev. D. 68 (2003) 124021

[37] Leeb., H., Schmiedmayer, J., Phys. Rev. Lett. 68 (1992) 1472

[38] Lambrecht, A., Reynaud, S., Eur. Phys. J. D 8 (2000) 309

[39] Long, J. C., Churnside, A. B., Price, J. C., Proc. Ninth Marcel Grossmann Mtg. on Gen. Rel. (World Scientific, 2002), part C, 1819-1825; hep-ph/0009062

[40] Harber, D. M., et al., Phys. Rev. A. 72 (2005) 033610.